Colloid Polym Sci (2012) 290:979–985
DOI 10.1007/s00396-012-2663-5

SHORT COMMUNICATION

Controlled preparation of core–shell polystyrene/polypyrrole nanocomposite particles by a swelling–diffusion–interfacial polymerization method

Zhen Huang · Chunjian Wang · Yunxing Li · Zhaoqun Wang

Received: 20 October 2011 / Revised: 20 March 2012 / Accepted: 15 April 2012 / Published online: 3 May 2012

Abstract Polystyrene/polypyrrole (PS/PPy) core–shell nanocomposite particles with uniform and tailored morphology have been successfully synthesized using the "naked" PS particulate substrate with the aid of a proposed strategy, the so-called swelling–diffusion–interfacial polymerization method. After initially forming pyrrole-swollen PS particles, diffusion of the monomer toward the aqueous phase was controlled through the addition of hydrochloric acid, eventually leading to its polymerization on the substrate particle surface. This process allows the nanocomposite particles to possess uniform and intact PPy overlayer and affords much more effective control over the structure and morphology of the resultant nanocomposites by simply changing the PS/pyrrole weight ratio or the addition amount of the doping acid. In particular, the nanocomposite particles with a thin, uniform, and intact PPy overlayer and their corresponding PPy hollow particles were obtained at a low addition amount of pyrrole. The resultant nanocomposite particles have been extensively characterized using scanning electron microscopy, transmission electron microscopy, Fourier transform infrared spectroscopy, Raman spectroscopy, and thermogravimetry.

Keywords Conducting polymer · Core–shell composite particle · Polypyrrole · Diffusion control · Interfacial polymerization

Z. Huang · C. Wang · Y. Li · Z. Wang (✉)
Department of Polymer Science and Engineering,
School of Chemistry and Chemical Engineering,
Nanjing University, Nanjing 210093, China
e-mail: zqwang@nju.edu.cn

Introduction

The past 10 years have witnessed increasing research activities centered on conducting polymer composites either in scientific or technological fields. Functional composite particles with tailored structures and morphologies have been prepared by various methods with organic or inorganic substrates [1–6].

Among them, coating polymer latex with a continuous overlayer of conjugated polymer and a core–shell structure has attracted intense interest, especially when polystyrene (PS) is used for the core since it is available at narrow size distributions over a wide size range (50 nm–10 μm), exhibiting tunable functionalities and excellent film-forming properties [7–13]. Polypyrrole (PPy) is an attractive one among the family of conductive polymers because of its associated electrical, electrochemical, and optical properties, coupled with excellent environmental stability. Such hybrid materials combine metallic-like conductivity with the processability of conventional polymers, which hence present them as potential materials suitable for applications in versatile fields such as electrochemical sensors, optoelectronic devices, and space science [14–18].

Latex particles coated by conducting polymer were first reported in 1987. Yassar et al. [19] reported that sulfonated and carboxylated PS could be coated with PPy overlayer using $FeCl_3$. This approach has found widespread attention following a series of studies [8, 20–24]. Armes' group demonstrated that micrometer-sized PS latex particles, stabilized by poly(*N*-vinylpyrrolidone), were successfully coated with PPy by in situ polymerization of pyrrole with $FeCl_3$ in aqueous solution. It was noted that only at low PPy loading

could uniform and well-defined composite particles be obtained [25, 26]. Then they attempted to coat the 130-nm diameter PS latex with PPy; unfortunately, the anticipated core–shell composite particles were not obtained. Instead, PPy was deposited as discrete 10- to 20-nm nanoparticles onto the PS surface, leading to irregular heteroflocculation [27]. Similarly, Wang et al. [28] synthesized PS latex surrounded by a corona of polyelectrolyte (e.g., polystyrene sulfonate) prior to the coating process, which was apparently adopted to take advantage of the electrostatic interaction with the positively charged PPy oligomers. Lee et al. [29] prepared PS/PPy nanocomposite particles by a one-step solution route in soap-free emulsion polymerization using hydrogen peroxide (H_2O_2) and a trace of ferric chloride ($FeCl_3$) as an initiator couple. Nevertheless, the size of the obtained nanocomposite particles was polydispersed with two peaks at about 250 and 420 nm.

Obviously, time-consuming surface modification complicates the synthetic procedure, while it could partly optimize the deposition architecture of the PPy overlayer. A facile approach of coating PPy onto substrates, regardless of other assistance, is still a scientific challenge.

Recently, we reported a considerably facile strategy, the so-called swelling–diffusion–interfacial polymerization method (SDIPM), for preparing PS/PANi and PS/PEDOT composite particles, aiming to improve and control their morphology and loading efficiency independent of surface pretreatments of the PS seed latex [30–33]. In the present work, we applied the distinct SDIPM to a PS–pyrrole system in which common PS microspheres without further surface functionalizations and modifications are chosen as seed particles to prepare PS/PPy composite particles with uniform morphology and controllable structure. Coating of the PS microspheres with polypyrrole is carried out through a process of preabsorbing pyrrole inside the PS particles and then driving its diffusion outwards and chemical oxidative polymerization on PS/water interface. Controlling over the structure and morphology of the PS/PPy nanocomposite particles is investigated by simply changing the amounts of addition of pyrrole. Besides, the influence of HCl/pyrrole molar ratio on the morphology and the PPy loading yield was discussed.

Experimental

Materials

Styrene (AR) and Pyrrole (AR) were purchased from Shanghai Chemical Reagent Co. and purified by distillation under reduced pressure. The purified monomer was kept at 4 °C until used. Potassium persulfate (KPS), of analytical reagent grade (Shanghai Chemical Reagent Co.), was purified by recrystallization in water. Ferric trichloride ($FeCl_3 \cdot 6H_2O$), hydrochloric acid, and tetrahydrofuran (THF) were purchased from Nanjing Chemical Reagent Co. and used as received. Distilled water was used for all reaction and treatment processes.

Synthesis of polystyrene seed particles

The PS latex was prepared by an emulsifier-free emulsion polymerization method. Water (140 mL) was added to a 250-mL four-necked round flask and heated to 70 °C. It was purged with nitrogen to eliminate the inhibiting effect of oxygen before the addition of styrene monomer under mechanical stirring. Following the attainment of a uniform dispersion, KPS dissolved in water (0.23 g/10 mL) was added. The polymerization was allowed to proceed under N_2 atmosphere for 24 h before cooling to room temperature.

Preparation of polystyrene/polypyrrole composite particles

Pyrrole was added to water at 0 °C and under ultrasonic treatment for 15 min, followed by the addition of the PS seed latex. The mixture was stirred with ultrasonic assistance for 30 min at 0 °C and then stirred in an ice bath for 5 h. The aqueous solution of $FeCl_3 \cdot 6H_2O$ was added to the dispersion in one batch; the initial $FeCl_3$/pyrrole molar ratio was fixed at 2.5:1. This was followed by the addition of hydrochloric acid (1 mol/L), in an equimolar amount relative to pyrrole, dropwise via syringe. The temperature was maintained at 0 °C for the first 4 h of polymerization, after which the polymerization was carried out for 20 h at room temperature. The content of the pyrrole monomer was kept constant at 0.1 g, and the weight ratio of the PS seed particle to pyrrole monomer was varied from 12:1 to 2:1. The resulting black PPy-coated PS latex was washed repeatedly by centrifugation until the supernatant became colorless. Finally, the product was dried in a dynamic vacuum oven for 48 h at room temperature.

Extraction of the PS core

Excess THF (10 mL) was added into 50 mg of the dried PS/PPy nanocomposite particles at room temperature. This dispersion was left overnight. The resulting black residue was filtered, washed with THF, and redispersed in water.

Characterization

The morphology of the PS seed particles and the resultant PS/PPy nanocomposite particles was observed both by scanning electron microscope (SEM) using an S-4800 instrument (Hitachi Co., Japan) operated at an accelerating voltage of 5 kV (samples not sputter-coated with gold prior to examination) and transmission electron microscopy

(TEM) using a JEM-100 CX (JEOL Co., Japan) microscope. Fourier transform infrared (FTIR) analysis was performed with a Bruker VECTORTM 22 FTIR spectrometer (Bruker Co., Germany). Raman spectra were measured using the MultiRam spectrometer (Bruker Co.). A continuous wave Nd:YAG laser working at 1,064 nm was employed for Raman excitation. A total of 200 scans were averaged in each spectrum obtained with a laser power of 10 mW. Thermogravimetric analysis (TGA) was conducted with a Pyris 1 TGA instrument (PerkinElmer Co., USA) at a heating rate of 20 °C/min in N_2 from room temperature up to 700 °C.

Results and discussion

The schematic process of preparing the PS/PPy nanocomposite particles is displayed in Fig. 1. In the initial stage, upon mixing pyrrole with the original seed latex, the former would be enriched inside the PS seed particles after a certain period according to their good affinity, eventually forming monomer-swollen seed particles. Pyrrole is distributed mainly in the solid seed particles, while the oxidant (i.e., $FeCl_3$), which is an integral component participating in the polymerization of the monomer, exists in the continuous phase. Hence, they could hardly react with each other at this stage. Following the change on factors of controlling the diffusion of the pyrrole from the solid phase toward the aqueous phase, the original thermodynamic equilibrium of the reactants between the two phases will be broken. During diffusion toward the aqueous phase, the pyrrole could encounter the oxidant $FeCl_3$ to initiate its chemical oxidative polymerization on the PS/water interface. Thus, the resultant PPy would yield readily coats on the seed particles simultaneously. This fabrication strategy was named as the "swelling–diffusion–interfacial polymerization method," which was proposed in our previous researches [30, 31]. As the formation proceeds, the swollen seed particles act as reservoirs that constantly release monomer to the external surface to keep the processes of diffusion and interface reaction going. In brief, the incorporation of PPy with the PS seed particles can be carried out with a unique "inside-out" manner, in contrast to the prevalent thinking toward random deposition or induced deposition. In the process, the outer surface of the seed particles is the necessary path where the diffusing monomer passes through. As a result, an overlayer of PPy can form more efficiently and controllably and, moreover, is very uniform independent of the surface modification or functionalization of the PS particles.

In our system, a good affinity of pyrrole with PS should lead to it being enriched inside the PS microspheres. Swelling of the PS latex with pyrrole was confirmed by the gradual disappearance of pyrrole droplets, which were initially visible under optical microscope observation. Therefore, numerous pyrrole-swollen PS particles formed in the system. By varying the PS/pyrrole weight ratio from 12:1 to 2:1, a series of PS/PPy composite particles was obtained; their SEM images are shown in Fig. 2. At a higher PS/pyrrole weight ratio, i.e., smaller amount of pyrrole, the resultant nanocomposite particles had a uniform and smooth surface, as shown in Fig. 2b, c. When adding the pyrrole to a larger amount, such as a PS/pyrrole weight ratio of 2:1, the nanocomposite particles still maintained their smooth spherical outline, though there was a mass of uniformly dispersed fine wrinkles on their surface, as displayed in Fig. 2d. In addition, their sizes were larger than that obtained by using smaller pyrrole amounts (Fig. 2b, c), suggesting that they possessed a thicker PPy shell. Even though very low pyrrole amounts were added, such as PS/pyrrole weight ratios of 12:1 and 6:1, the resulting nanocomposite particles possessed very thin but intact and firm PPy shell. As shown in Fig. 2e, f, PPy hollow particles were obtained after extraction treatment of the composite particles. Some less uniform small particles were observed on the PPy hollow particles (Fig. 2f), and by comparing the hollow particles with their PS/PPy composite counterparts, it is logical to consider that they could be derived from reprecipitation of the residual PS chains that were unseparated from the medium and attached to the particle surface. These two kinds of well-shaped PPy hollow particles had very thin walls, but differentiable thickness (about 10 and 20 nm, respectively), thus directly reflecting the difference in thickness of the PPy overlayer of the PS/PPy nanocomposite particles; this difference was hardly distinguished according to their

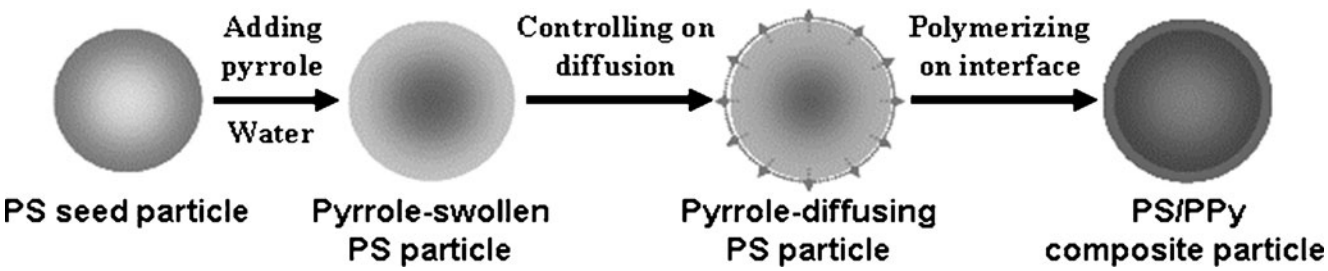

Fig. 1 Schematic representation of preparing PS/PPy nanocomposite particles using the swelling–diffusion–interfacial polymerization method

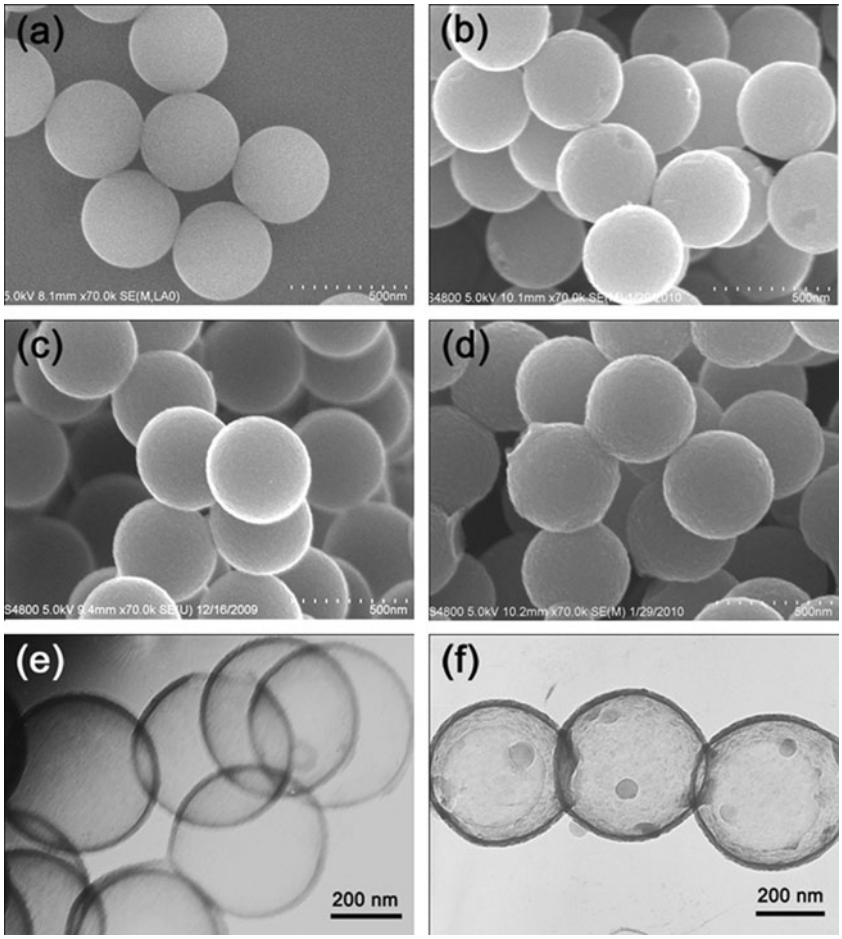

Fig. 2 SEM images of PS seed particles (**a**) and PS/PPy nanocomposite particles prepared with different PS/pyrrole weight ratios: 12:1 (**b**), 6:1 (**c**), and 2:1 (**d**), respectively. TEM images of the remaining PPy residue derived from the extraction treatment of PS/PPy nanocomposite particles prepared with PS/pyrrole weight ratios of 12:1 (**e**) and 6:1 (**f**)

diameters in the SEM images. Therefore, the PPy shell thickness can be effectively tuned by simply changing the PS/pyrrole weight ratio. What is more is that the uniform thickness of the PPy overlayer was obtained at such a low level of added pyrrole, even on the surface of "naked" PS particles. This also suggests a higher efficiency of transforming the initially added pyrrole into PPy in the nanocomposite particles at its low added amount. Together with all the results mentioned above, therefore, we could come to the conclusion that not only the uniform and smooth but also intact and hard PPy overlayers were formed on the surface of "naked" PS particles without any surface modifications. All of these should benefit from the distinct SDIPM, by which the incorporation of PPy into the PS particles can be carried out with the unique "inside-out" manner, an outstanding advantage of the SDIPM compared with the widely used conventional synthetic protocols.

The FTIR spectra of this series of PS/PPy nanocomposite particles definitely exhibit the varied thickness of PPy overlayers observed in the above TEM images. As shown in c–e in Fig. 3, for all the nanocomposites prepared using different PS/Pyrrole weight ratios of 12:1, 6:1, and 2:1, the absorption bands appear notably at 1,549, 1,316, 1,186, and 910 cm^{-1}, in addition to the characteristic peaks of PS (i.e., 1,565, 1,487, 756, and 698 cm^{-1}). They can be attributed to the PPy component by using the bulk PPy spectrum (b in Fig. 3) as a reference. The arisen band intensities of the characteristic peaks of the PPy component are regarded as a supporting evidence for the core–shell morphology.

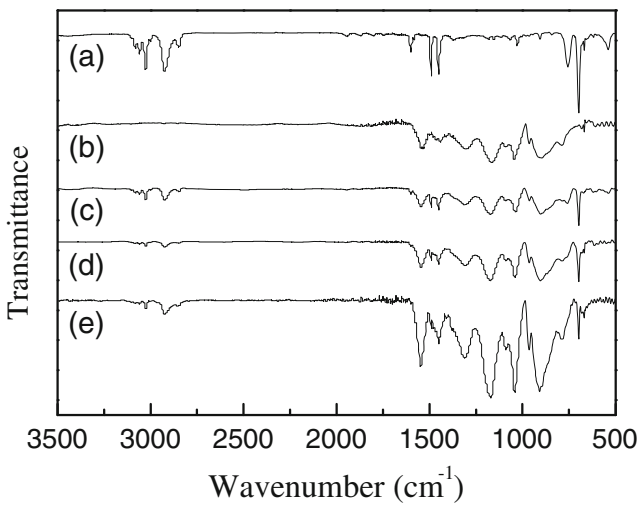

Fig. 3 FTIR spectra of PS seed particles (*a*), PPy bulk powder (*b*), and PS/PPy nanocomposite particles with different PS/pyrrole weight ratios: 12:1 (*c*), 6:1 (*d*), and 2:1 (**e**)

Moreover, it is clear that the intensities enhance proportionally to the increase of the initial amount of added pyrrole (from curve c to e), increasingly obscuring the underlying PS cores by PPy overlayers. Accordingly, it demonstrates the gradual thickening of PPy overlayers.

The Raman spectra of the original PS particles, a heterogeneous admixture of PS and PPy (9:1, *w*/*w*) and PS/PPy nanocomposite particles, are depicted in Fig. 4. The PS component has a very strong signal at approximately 1,002 cm^{-1} (curve a, v_1 ring-breathing mode), which is in excellent agreement with the Raman spectra of PS reported by previous workers [25]. However, this strong signal completely disappears (curve c) when the PS was coated by a thin PPy overlayer for the sample shown in Fig. 2b, e. This spectrum is just identical to that of pure polypyrrole (omitted here), in sharp contrast with the control sample, i.e., the heterogeneous admixture of PS and PPy (9:1 *w*/*w*). In the latter case, the signals belonging to the PS are readily observed (curve b), even though the admixture has a much lower PS weight percentage content than the PS/PPy nanocomposite particles. This phenomenon can be regarded as a powerful evidence for the PS/PPy core–shell structure because the Raman signals attributed to the PS core could be attenuated or absorbed by the PPy overlayer when it completely enveloped the PS and simultaneously has a certain thickness [25, 34, 35].

In accordance with the TGA curves shown in Fig. 5, the PS seed particles start their weight loss at ~350 °C and are completely decomposed at ~450 °C (curve e), whereas the PPy bulk powder gradually loses weight with a linear trend line (curve a). For the nanocomposite particles, there are two decomposition onsets in the TGA curves b, c, and d, which reflect that each component maintains independent domains

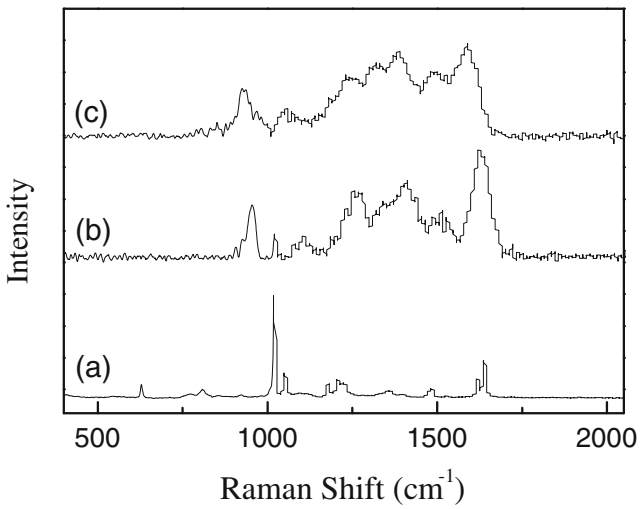

Fig. 4 Raman spectra of PS seed particles (*a*), a heterogeneous admixture of 10 wt% PPy and 90 wt% PS (*b*), and PS/PPy nanocomposite particles prepared with a PS/pyrrole weight ratio of 12:1 (*c*)

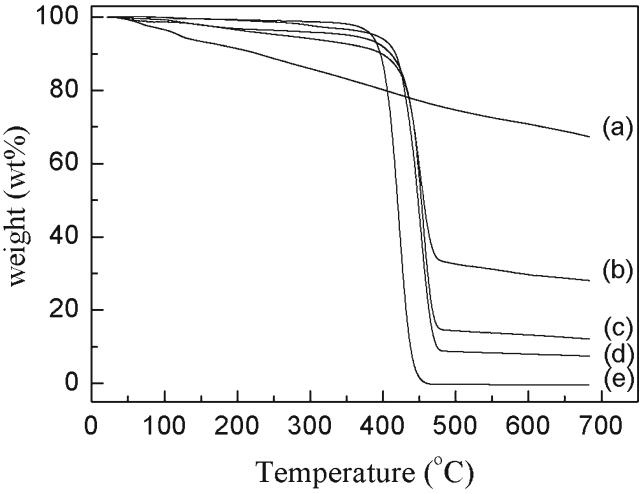

Fig. 5 TGA curves of PPy bulk powder (*a*), PS/PPy composite particles prepared with different PS/pyrrole weight ratios of 2:1 (*b*), 6:1 (*c*), and 12:1 (*d*), and PS seed particles (*e*)

inside the nanocomposite particles. Moreover, it is noteworthy that the complete decomposition temperature increased from 450 °C of the original PS particles to 480 °C for all the PS/PPy nanocomposite particles. This improvement can be attributed to a restriction of the PPy overlayer on the diffusion of PS oligomers/monomer produced by decomposition [36]. Both provide further evidence for the formation of core–shell morphology. On the other hand, the first decomposition platforms move downward more noticeably from curve d to curve b. It means a gradual enlargement of the PPy domains with increasing initial amount of added pyrrole based on the gradual decomposition of PPy starting before the first inflection temperature. Correspondingly, the height of the second platforms, attributable to the residue of the PPy parts, shows a completely opposing trend. These two different trends before and after PS decomposed exactly reveal the same fact that the thickness of the PPy overlayer increases steadily in accordance with an increased amount of initially added pyrrole. As TGA experiments were conducted in N_2 atmosphere, the PPy could be transformed into carbon-rich materials rather than completely decomposed [37], in agreement with the fact that there is only a weight loss of ~33 % at 700 °C (curve a). According to these TGA results, together with the empirical composition of doped PPy [38], the loading efficiency of PPy onto PS seed particles, namely, the ratio of PPy actual content incorporated into the nanocomposite particles to the theoretical one (related to the initial PS/pyrrole weight ratio), can be determined to be 78.3, 79.0 and 92.7 %, corresponding to the initial PS/pyrrole weight ratios of 2:1, 6:1, and 12:1, respectively. In other words, the greatest conversion efficiency of pyrrole can be achieved at the lowest added amount even on the "naked" PS seed particles without further surface modifications, which is precisely an outstanding advantage of

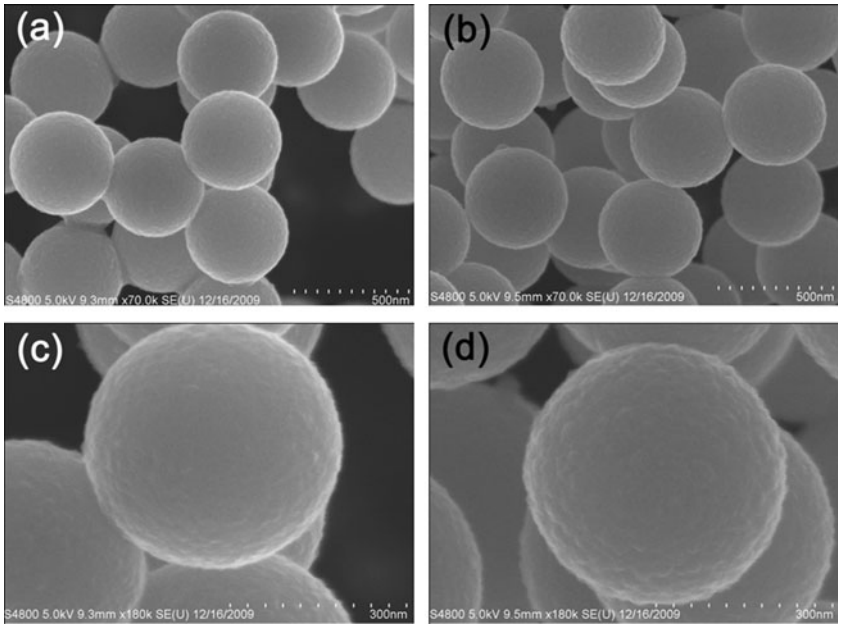

Fig. 6 SEM images of PS/PPy nanocomposite particles prepared using the same PS/pyrrole weight ratio of 6:1, but different HCl addition amounts of 0 ml (**a**, **c**) and 12.5 ml (**b**, **d**)

the SDIPM compared with traditional induced deposition method. This is also the reason for successfully obtaining the smooth PPy overlayers and then the intact PPy hollow particles with thin walls (as shown in Fig. 2b, e) at very low concentrations of pyrrole. With decreasing PS/pyrrole weight ratio (i.e., increasing amount of added pyrrole), the loading efficiency declines, but still maintains a relatively high value above 78 %. Furthermore, the PS/PPy nanocomposite particles are still provided with the uniform outline and well-defined morphology even up to a PS/pyrrole weight ratio of 2:1.

According to the formation mechanism of the resultant nanocomposite particles and our previous works, an alternative way to drive the diffusion of preabsorbed monomer, and thus to control the structure of the nanocomposite particles, is to vary the addition rate of doping acid. SEM images corroborate that the addition of a HCl solution has an important effect on the morphology of the resulting PPy overlayer. Compared with the smooth ones prepared without adding a HCl solution (Fig. 6a, c), the nanocomposite particles exhibit an obviously rougher overlayer at 12.5 ml of HCl ($n_{HCl}/n_{pyrrole}$, molar ratio of HCl/pyrrole of 100:1; Fig. 6b, d). Figure 7 shows the loading yield of PPy into nanocomposite particles (i.e., the loading efficiency) obtained with different amounts of addition of HCl, which was determined by thermogravimetric analysis. With an increase in the HCl amount, PPy loading yields increase sharply at the beginning and then immediately reach an approximate plateau of about 85 %. The steep rise of loading yield at low $n_{HCl}/n_{pyrrole}$ proves that the addition of HCl is crucial to drive the outward diffusion of the preabsorbed pyrrole and, thus, to start its interface polymerization, which agrees well with the SDIPM mechanism. From the viewpoint of match between the diffusion and polymerization of the monomer, the loading yield will no longer be sensitive to the addition amount of acid at its higher level because it has reached an adequate diffusion capability of the preabsorbed pyrrole. At the same time, a stronger outward diffusion of pyrrole could lead to the rougher PPy overlayer, as depicted in Fig. 6d.

Conclusion

In conclusion, monodisperse PS/PPy core–shell nanocomposite particles were controllably fabricated using the ordinary "naked" PS seed particles without further surface

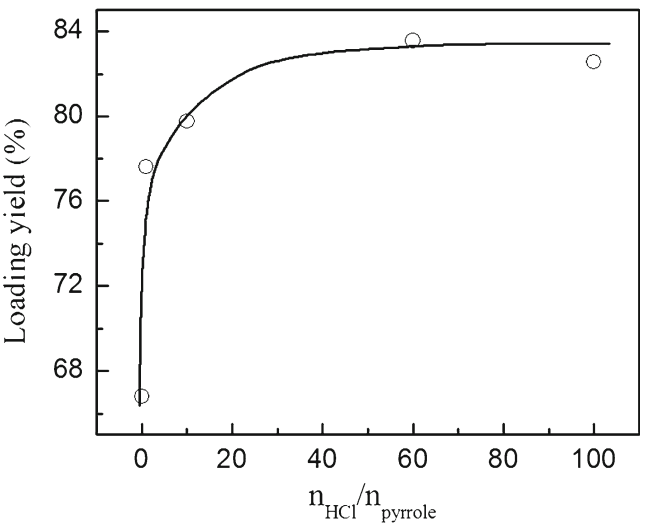

Fig. 7 PPy loading yield of the PS/PPy nanocomposite particles prepared using different amounts of addition of HCl

modifications with the aid of the proposed SDIPM. The formation of the thin but uniform, intact PPy overlayer profited from the unique "inside-out" forming process and the considerably high efficiency of loading pyrrole on the PS particles. At a larger amount of addition of pyrrole, there was a relatively high PPy mass loading yields and the PS/PPy nanocomposite particles still possessed the uniform size and well-defined morphology. Correspondingly, profiting from the high transform efficiency of pyrrole and uniform coating of PPy, very thin but well-shaped PPy hollow particles were prepared. To be brief, the SDIPM can be applied validly for such ordinary PS particles, and we can give powerful control over the structure and morphology of the PS/PPy core–shell nanocomposite particles by simply changing the PS/pyrrole weight ratio or the addition amount of the doping acid.

Acknowledgments This work was supported by the National Natural Science Foundation of China (no. 51133002).

References

1. Gangopadhyay R, De A (2000) Chem Mater 12(3):608–622
2. Gomez-Romero P (2001) Adv Mater 13(3):163–174
3. Li WG, McCarthy PA, Liu DG, Huang JY, Yang SC, Wang HL (2002) Macromolecules 35(27):9975–9982
4. Thiyagarajan M, Samuelson LA, Kumar J, Cholli AL (2003) J Am Chem Soc 125(38):11502–11503
5. Roux S, Soler-Illia GJAA, Demoustier-Champagne S, Audebert P, Sanchez C (2003) Adv Mater 15(3):217–221
6. Percy MJ, Michailidou V, Armes SP, Perruchot C, Watts JF, Greaves SJ (2003) Langmuir 19(6):2072–2079
7. Nazar LF, Zhang Z, Zinkweg D (1992) J Am Chem Soc 114 (15):6239–6240
8. Khan MA, Armes SP (2000) Adv Mater 12(9):671–674
9. Kim JW, Larsen RJ, Weitz DA (2006) J Am Chem Soc 128 (44):14374–14377
10. Bromley CWA (1986) Colloids Surf 17(1):1–11
11. Goodall AR, Wilkinson MC, Hearn J (1977) J Polym Sci Polym Chem 15(9):2193–2218
12. Ramanavicius A, Ramanaviciene A, Malinauskas A (2006) Electrochim Acta 51(27):6025–6037
13. Caruso F, Caruso RA, Mohwald H (1998) Science 282 (5391):1111–1114
14. Mangeney C, Fertani M, Bousalem S, Zhicai M, Ammar S, Herbst F, Beaunier P, Elaissari A, Chehimi MM (2007) Langmuir 23 (22):10940–10949
15. Madani A, Nessark B, Brayner R, Elaissari H, Jouini M, Mangeney C, Chehimi MM (2010) Polymer 51(13):2825–2835
16. Lu Y, Pich A, Adler HJP, Wang G, Rais D, Nespurek S (2008) Polymer 49(23):5002–5012
17. Goldsworthy BJ, Burchell MJ, Cole MJ, Armes SP, Khan MA, Lascelles SF, Green SF, McDonnell JAM, Srama R, Bigger SW (2003) Astron Astrophys 409(3):1151–1167
18. Bousalem S, Yassar A, Basinska T, Miksa B, Slomkowski S, Azioune A, Chehimi MM (2003) In: Synthesis, characterization and biomedical applications of functionalized polypyrrole-coated polystyrene latex particles. 2nd International Conference on Modification, Degradation and Stabilization of Polymers, Budapest, Hungary, 2002, 2003. Wiley, Budapest, Hungary, pp 820–825
19. Yassar A, Roncali J, Garnier F (1987) Polym Commun 28(4):103–104
20. Armes SP, Gottesfeld S, Beery JG, Garzon F, Agnew SF (1991) Polymer 32(13):2325–2330
21. Liu CF, Maruyama T, Yamamoto T (1993) Polym J 25(4):363–372
22. Lascelles SF, Armes SP (1995) Adv Mater 7(10):864–866
23. Huijs FM, Vercauteren FF, de Ruiter B, Kalicharan D, Hadziioannou G (1999) Synth Met 102(1–3):1151–1152
24. Fujii S, Armes SP, Jeans R, Devonshire R, Warren S, McArthur SL, Burchell MJ, Postberg F, Srama R (2006) Chem Mater 18 (11):2758–2765
25. Lascelles SF, Armes SP, Zhdan PA, Greaves SJ, Brown AM, Watts JF, Leadley SR, Luk SY (1997) J Mater Chem 7 (8):1349–1355
26. Lascelles SF, Armes SP (1997) J Mater Chem 7(8):1339–1347
27. Cairns D, Armes S, Bremer L (1999) Langmuir 15(23):8052–8058
28. Wang JJ, Sun L, Mpoukouvalas K, Lienkamp K, Lieberwirth I, Fassbender B, Bonaccurso E, Brunklaus G, Muehlebach A, Beierlein T, Tilch R, Butt HJ, Wegner G (2009) Adv Mater 21(10–11):1137–1141
29. Lee JM, Lee DG, Lee SJ, Kim JH, Cheong IW (2009) Macromolecules 42(13):4511–4519
30. Li YX, Wang ZQ, Wang Q, Wang CJ, Xue G (2010) Macromolecules 43(10):4468–4471
31. Wu Q, Wang ZQ, Xue G (2007) Adv Funct Mater 17(11):1784–1789
32. Li YX, Wang ZQ, Wang CJ, Zhao Z, Xue G (2011) Polymer 52 (2):409–414
33. Yin DP, Li YX, Huang Z, Gu H, Wang ZQ (2011) Polymer 52 (21):4785–4791
34. Barthet C, Armes SP, Lascelles SF, Luk SY, Stanley HME (1998) Langmuir 14(8):2032–2041
35. Jenden CM, Davidson RG, Turner TG (1993) Polymer 34 (8):1649–1652
36. Fujii S, Matsuzawa S, Nakamura Y, Ohtaka A, Teratani T, Akamatsu K, Tsuruoka T, Nawafune H (2010) Langmuir 26 (9):6230–6239
37. Han CC, Lee JT, Yang RW, Chang H, Han CH (1998) Chem Commun 1998(19):2087–2088
38. Mathys GI, Truong VT (1997) Synth Met 89(2):103–109